Journal of Hazardous Materials 191 (2011) 126–135

Contents lists available at ScienceDirect

Journal of Hazardous Materials

journal homepage: www.elsevier.com/locate/jhazmat

Enhancing atrazine biodegradation by *Pseudomonas* sp. strain ADP adsorption to Layered Double Hydroxide bionanocomposites

Tatiana Alekseeva[a,b,c], Vanessa Prevot[b,d], Martine Sancelme[c], Claude Forano[b,**], Pascale Besse-Hoggan[c,e,*]

[a] Institute of Physical, Chemical and Biological Problems of Soil Science, Russian Academy of Sciences, Pushchino, Moscow Region 142290, Russia
[b] Clermont Université, Université Blaise Pascal, Laboratoire des Matériaux Inorganiques, BP 80026, 63171 Aubière Cedex, France
[c] Clermont Université, Université Blaise Pascal, Laboratoire de Synthèse et Etude de Systèmes à Intérêt Biologique, BP 80026, 63171 Aubière Cedex, France
[d] CNRS, UMR 6002, Laboratoire LMI, 63177 Aubière Cedex, France
[e] CNRS, UMR 6504, Laboratoire SEESIB, 63177 Aubière Cedex, France

ARTICLE INFO

Article history:
Received 7 February 2011
Received in revised form 11 April 2011
Accepted 12 April 2011
Available online 19 April 2011

Keywords:
Layered Double Hydroxides
Humic acid–LDH complexes
Pseudomonas sp. strain ADP
Bacteria adsorption
Atrazine
Biodegradation rate

ABSTRACT

To mimic the role of hydroxide minerals and their humic complex derivatives on the biodegradability of pesticides in soils, synthetic Mg_RAl Layered Double Hydroxides (LDH) and Mg_RAl modified by Humic substances (LDH–HA) were prepared for various *R* values (2, 3 and 4) and fully characterized. Adsorption properties of LDH and LDH–HA toward *Pseudomonas* sp. strain ADP were evaluated. The adsorption kinetics were very fast (<5 min to reach equilibrium). The adsorption capacities were greater than previously reported (13.5×10^{11}, 41×10^{11} and 45.5×10^{11} cells/g LDH for Mg_2Al, Mg_3Al and Mg_4Al, respectively) and varied with both surface charge and textural properties. Surface modification by HA reduced the adsorption capacities of cells by 2–6-fold. Biodegradation kinetics of atrazine by *Pseudomonas* sp. adsorbed on both LDHs and LDH–HA complexes were measured for various solid/liquid ratios and adsorbed cell amounts. Biodegradation activity of bacterial cells was strongly boosted after adsorption on LDHs, the effect depending on the quantity and properties of the LDH matrix. The maximum biodegradation rate was obtained in the case of a 100 mg/mL Mg_2Al LDH suspension (26 times higher than that obtained with cells alone).

1. Introduction

To treat organic contamination in natural environments or in specific industrial effluent treatment plants, biological processes have gained interest due to their eco-friendly and cost-effective aspects. Nevertheless, bioremediation techniques can lead to currently unpredictable results in terms of effectiveness and clean-up time [1–4].

In natural environments, bacteria tend to attach to solid surfaces. This prevailing microbial state, known as biofilm, confers protection against environmental stresses and increases their survival [5,6]. Bacteria adsorption was studied and compared on various surfaces [7–14]. The results show that adhesion occurs on all types of surfaces and it is affected by mineral, bacteria cell surface properties and the characteristics of fluid phase (pH, ionic strength). As described by DLVO theory of colloid stability [15], two main types of interaction between bacteria and mineral solids are involved: van der Waals attraction and electrostatic interactions that are generally repulsive [10,16]. Besides, bacteria adhesion is influenced by the hydrophobicities of both cells and solids, the bacteria extracellular structures and the presence of divalent cations providing additional bridging.

There is an agreement in the literature that bacterial attachment to the support could influence their metabolic activity although the effect is often controversial [17–22]. The effect of microbial adhesion on substrate has been attributed to the creation of microenvironments at the surface favourable to its metabolic activity by buffering the medium [17,19] or to the substrate sorption allowing a direct access at a short distance for the microorganism to the compounds [23].

Recently, Besse-Hoggan et al. [24] found that the biodegradation of atrazine (AT) by *Pseudomonas* sp. strain ADP was dramatically enhanced in the presence of $Mg_2Al(OH)_6NO_3{\cdot}nH_2O$ hydrotalcite like compound (Layered Double Hydroxides or LDH) although AT was not sorbed on this inorganic matrix. A few other papers

* Corresponding author at: Laboratoire de Synthèse Et Etude de Systèmes à Intérêt Biologique, UMR-CNRS 6504, Université Blaise Pascal, BP 80026, 63171 Aubière Cedex, France. Tel.: +33 04 73 40 71 21; fax: +33 04 73 40 77 17.
** Corresponding author at: Laboratoire des Matériaux Inorganiques, UMR-CNRS 6002, Université Blaise Pascal, BP 80026, 63171 Aubière Cedex, France. Tel.: +33 04 73 40 73 35; fax: +33 04 73 40 71 08.
E-mail addresses: Claude.Forano@univ-bpclermont.fr (C. Forano), Pascale.Besse@univ-bpclermont.fr (P. Besse-Hoggan).

0304-3894/$ – see front matter © 2011 Elsevier B.V. All rights reserved.
doi:10.1016/j.jhazmat.2011.04.050

have reported that microorganisms can strongly interact with LDH [7,25], the purpose of all these experiments being to set up efficient anti-microbial processes or wastewaters treatments. LDH is a class of ionic lamellar minerals with positively charged hydroxylated layers of divalent and trivalent metallic cations ($[M^{II}_{1-x}M^{III}_{x}(OH)_2]^{x+}$) and exchangeable hydrated gallery anions ($[X^{q-}_{x/q}\cdot nH_2O]$) [26]. The neoformation of LDH may occur in alkaline soils [27–31] and they can be regarded as good representatives of the oxide/hydroxide soil mineral family.

The purpose of this study is to evaluate the key parameters governing the bacteria-LDH adhesion and how it can influence the biodegradation of a non-sorbed pesticide, atrazine. For that, LDH with different Mg/Al ratios were synthesized to investigate the effect of LDH surface properties (ζ-potential, particle size, surface charge density) on cell adsorption and evaluated for the subsequent effect on AT biodegradation. The influence of modification of LDH surface by adsorbed humic acid (HA) was also studied.

2. Materials and methods

2.1. Preparation and characterization of materials

Synthetic nitrate intercalated LDH with 2, 3 and 4 mg/Al molar ratios (noted hereafter Mg_2Al, Mg_3Al and Mg_4Al) were prepared by the co-precipitation method at a controlled pH of 9.0 according to de Roy et al. [32] and Chang et al. [33]. LDH products were used as aqueous suspensions obtained either directly from synthesis (undried samples) or from re-suspended air-dried solids. Humic acid Na-salt (HA) was purchased from Aldrich. LDH–HA complexes were laboratory prepared based on HA adsorption isotherms, as described previously [24]. The X-ray diffraction patterns of the solids were recorded with a Philips X'Pert automated X-ray diffractometer using Cu Kα radiation (λ = 0.154051 nm), over the 2–70° (2θ) range in steps of 0.0668° with a counting time per step of 4 s. FT-IR spectra were recorded with a Nicolet 5700 spectrometer from ThermoElectron Corporation using the KBr pellet technique; particle sizes and Zeta-potentials were measured with the nano Zeta-sizer (Malvern instruments) apparatus. The bacteria–LDH assemblies were studied by transmission electron microscopy (TEM) using a Hitachi 7650 microscope at an acceleration voltage of 80 kV. To perform the characterization, a drop of the suspension was deposited on a 400 mesh holey carbon-coated copper grid and dried at room temperature.

2.2. Preparation of the cell suspension

Pseudomonas sp. strain ADP (gift from Dr F. Martin-Laurent) was grown in 100 mL portions of Trypticase Soy broth in 500 mL Erlenmeyer flasks incubated at 27 °C and 200 rpm. The cells were prepared as previously described [24].

2.3. Sorption isotherms

Pseudomonas sp. adsorption onto solids was carried out using the batch-equilibration technique at 20 °C. The reactive volume (3 mL in plastic cuvettes) contained a solid suspension at a 500 mg/L concentration and cells within a range from 0.06 to 1.25×10^{10} mL^{-1} (10 point isotherms). The solid was pre-conditioned overnight in Volvic water (pH 7) to obtain a homogeneous suspension. After addition of the bacterial suspension in the cuvette, the mixture was stirred for 15 min and then left for sedimentation for a 4 h period. Supernatants were then analyzed by UV spectroscopy (Nicolet evolution 500 spectrometer, Thermo Electron Corporation) at 600 nm to determine the amount of cells left in the equilibrium solution. Blanks were carried out with LDH or LDH–HA complex suspensions under the same conditions and their absorbance values have been taken into account for isotherm calculations. Adsorption isotherms were processed from 2 to 4 independent experiments. The amount of cells adsorbed was calculated as the difference between initial and equilibrium cell concentrations per gram of the solid.

Adsorption of AT by cells or cell-LDH was controlled. After centrifugation and removal of the supernatant, the bacterial pellet or the (bacterial-sorbent LDH) pellet was resuspended in a mixture $MeOH/H_2O$ 4/1 and stirred vigorously for 24 h in order to extract AT and its metabolite that could be adsorbed on the cells or remained in the cells. This experiment was carried out on several samples taken during the AT biodegradation. None of the extracts contained AT or OH-AT. The free or immobilized cells do not adsorb AT. This was not the case for Mg_RAl HA complexes on which AT and OH-AT were adsorbed and were found in great quantity after extraction.

2.4. Biodegradation experiments

To work under the same conditions as those used for sorption experiments, a two-step process was carried out: after a 24 h period of contact between the solid matrix (100, 250, 500 or 1000 mg) and a 0.1 mM AT solution in Volvic® water (5 mL) in 100 mL flasks on a platform shaker (200 rpm, 27 °C) (homogenization step), a resting-cell suspension of *Pseudomonas* sp. ADP (resuspension of the pellet (55 mg dry weight) in 5 mL of a 0.1 mM AT solution), was introduced (incubation step). A control of AT biodegradation in aqueous medium (10 mL) was carried out in each series of experiments to compare kinetics appropriately. The blanks consisted of preparations incubated under the same conditions without AT or cells. Samples (1 mL) were regularly taken from each flask, centrifuged at 12,500 rpm for 3 min and then frozen till HPLC analyses. All these experiments were repeated at least 3 times.

Hydroxyatrazine (OH-AT), the first metabolite of the atrazine (AT) biodegradation pathway by *Pseudomonas* sp. strain ADP, was detected in all the experiments (monitored by HPLC), showing clearly that the bacterial cells were metabolically active. This metabolite disappeared rapidly from the supernatant in the presence of LDHs (after 2 h of incubation *vs* 35 h with cells alone). We have checked that OH-AT was not adsorbed on LDHs.

2.5. Atrazine HPLC analyses

Supernatants were analyzed by HPLC at 22 °C using an Agilent 1100 photodiode array detector (DAD) chromatograph. A reversed-phase column (Zorbax Eclipse XDB-C18, 5 μm, 150 mm × 4.6 mm) was used at a flow rate of 1 mL/min. The mobile phase was composed of 50 mM acetate buffer pH 4.6 and acetonitrile 60/40 (v/v). The injection volume was 10 μL. The UV detector was set at 225 nm.

2.6. Statistical data processing

Statistical processing of the obtained data has been done using "STATISTICA" program (StatSoft, Inc., version 8.0, 2007; www.statsoft.com).

3. Results

3.1. Properties of LDH and LDH–HA complexes

The XRD data (Fig. 1A) of the three synthetic inorganic compounds (Mg_RAl) confirmed the formation of pure nitrate intercalated LDH phases displaying a hexagonal lattice with a rhombohedral symmetry ($R\bar{3}m$). Refined cell parameters are equal to a = 3.036(4) nm, 3.058(4) nm and 3.075(3) nm and c = 0.8856(6) nm, 0.8509(7) nm and 0.7917(6) nm for Mg_RAl with

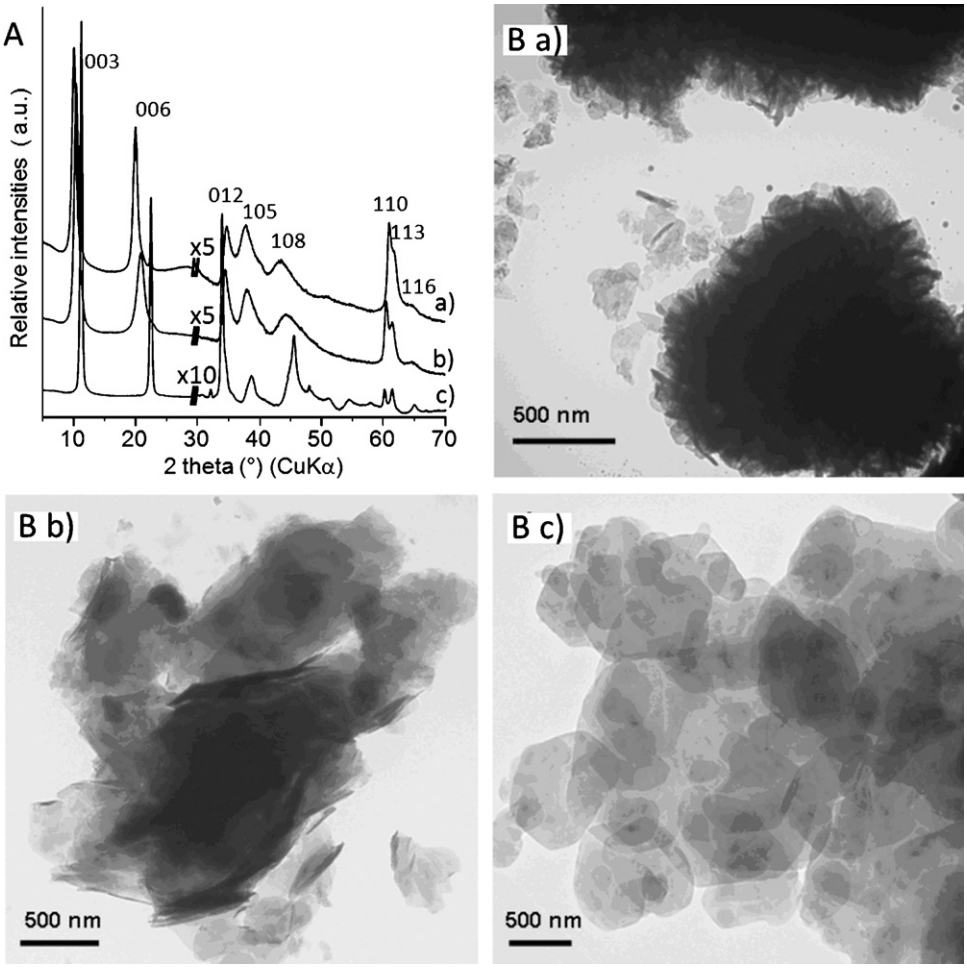

Fig. 1. PXRD (A) and TEM images (B) of (a) Mg_2Al, (b) Mg_3Al and (c) Mg_4Al.

R equal to 2, 3 and 4, respectively. Chemical analyses gave experimental *R* = Mg/Al molar ratios of 1.95, 2.66 and 4.07, very close to the desired chemical compositions (referred to as Mg_2Al, Mg_3Al and Mg_4Al), allowing to study the effect of anion exchange capacity on cell adsorption. Particle size and zeta-potential (ζ) of all studied solids are given in Table 1. The particle size of LDH series (dried and undried samples) showed opposite tendencies: it decreased with the Mg/Al ratio for Mg_RAl kept in suspension while it increased for dried Mg_RAl. The zeta-potentials of all LDH precursors were positive and visibly larger for undried samples. Adsorption of HA at the LDH surface resulted first in a clear decrease of the particle size of the precursors due to a partial exfoliation of the materials and second in a charge inversion of the solid surface. Further experiments performed on Mg_3Al showed that the negative zeta-potential values increased continuously with the HA percentage (Table 1).

Table 1
Particle size and zeta-potential of LDH, LDH–HA complexes and cells.

Samples		Particle size, nm	ζ, mV
	Dry	3812	+6.1 ± 0.1
Mg_2Al	ud.[a]	1563	+23.7 ± 0.2
	+10% HA	1990	−18.4 ± 0.4
	Dry	5445	+12.0 ± 0.5
	ud.[a]	1387	+26.8 ± 0.2
Mg_3Al	+2% HA	2456	−11.1 ± 0.4
	+10% HA	1718	−19.4 ± 0.5
	+20% HA	1727	−24.4 ± 0.4
	Dry	8594	+6.4 ± 0.1
Mg_4Al	ud.[a]	957	+27.1 ± 0.2
	+10%HA	1700	−29.6 ± 0.7
Pseudomonas sp. strain ADP		1280–1990	−19.0 ± 0.5

[a] ud.: undried products.

TEM images of the different dried LDHs are shown in Fig. 1B. Images suggest that precursors have a quite different morphology. Although all materials are formed of nanosized platelets, they grew or were associated in different ways. Mg_2Al (Fig. 1B, a) display small primary particles (50–200 nm) aggregated into the so-called "sand rose" morphology with size of about 1–2 μm, each of them being formed from the association of 3, 5 or much more individual spherical "roses" (detailed structure on Fig. 1B, a). In comparison, LDH with Mg/Al ratio of 3 and 4 display larger platelets and aggregates (Fig. 1B, b and c), as confirmed by dynamic light scattering (DLS) measurements (Table 1). Well-defined hexagonal plate-like particles with particle size in the range from 0.1 to 1.5 μm are only observed for Mg_4Al phase, the thin flake primary particles being stacked together. Note that all the compounds display similar BET surface area, in the range of 25–35 m^2/g (data not shown).

For undried LDH samples, particle sizes are smaller due to the limitation of platelet aggregation. For Mg_4Al, primary particle sizes observed by TEM (780–930 nm) are in good agreement with the size measured by DLS (957 nm). Agglomeration is totally avoided in this case. While for Mg_2Al and Mg_3Al suspensions, aggregation of single particles occurs but is strongly reduced due to the absence of drying.

In conclusion, the decrease in primary particles size in the series $Mg_4Al > Mg_3Al > Mg_2Al$ leads to bigger aggregates or secondary

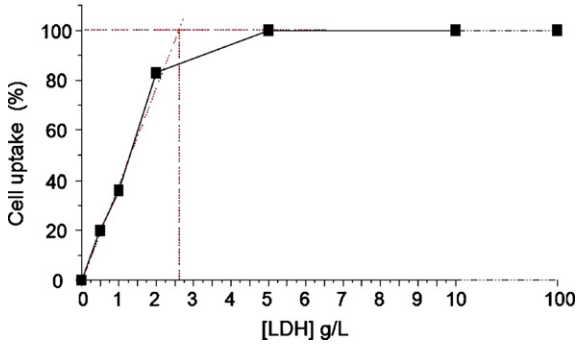

Fig. 2. Effect of Mg_3Al LDH concentration on cell adsorption percentage. Cell concentration: 1.25×10^{10} mL^{-1}.

particles. Drying obviously has a major effect on the aggregation of Mg_4Al single particles and will probably affect adsorption properties. It leads to bigger face to face packing while once the aggregation is already advanced (*i.e.* Mg_2Al sand roses like particles), less evolution of the particle size can be expected.

3.2. *Pseudomonas sp. sorption onto LDH and LDH–HA complexes*

The adsorption capacity of the different Mg_RAl LDH has been first investigated for a bacteria concentration of 1.25×10^{10} mL^{-1} and a wide range of solid concentrations (0.5–100 g/L) using the batch-equilibration technique. A preliminary kinetical study of sedimentation of bacterial cells, LDH and LDH–HA complexes showed that cell suspensions were stable for at least a 5 h period whatever their concentrations (Supporting information, Fig. S1a). Conversely, LDH and LDH–HA suspensions showed rapid sedimentation; even though a greater stability was observed for complex suspensions (Supporting information, Fig. S1b). *Pseudomonas* sp. sorption onto both LDH and LDH–HA complexes is instantaneous and no desorption has been observed after vigorous stirring of LDH/bacteria mixture for up to 60 min (data not shown).

Results of adsorption for the considered cell concentration showed that the cell uptake increases as more Mg_RAl adsorbent is used. The example of Mg_3Al is given in Fig. 2. In all cases, 100% of the cells were adsorbed for LDH amount greater than 5 g/L. For the lowest solid concentration (0.5 g/L), an effect of the LDH Mg/Al ratio was observed; Mg_2Al, Mg_3Al and Mg_4Al adsorbed respectively 5%, 20% and 21% of the initial cell concentration. Before saturation, cell uptake was linearly dependent on the solid amount. The bacteria removal efficiency corresponds to 13.5×10^{11}, 41×10^{11} and 45.5×10^{11} cells/g for Mg_2Al, Mg_3Al and Mg_4Al, respectively.

Adsorption isotherms of cells for dried and undried LDHs and dried LDH/HA complexes (500 mg/L) are given in Fig. 3. All isotherms belong to the H-type, *i.e.* cells have a high affinity for supports. For dried LDHs (Fig. 3a–c) at low cell concentrations ($0.125–0.375 \times 10^{10}$ mL^{-1}), 100% of cells were sorbed; when the cell concentration increased ($0.375–1.250 \times 10^{10}$ mL^{-1}), isotherms showed a plateau corresponding to the saturation stage, as stated by the Langmuir model for molecular adsorption. The adsorption capacity, determined at the plateau (Fig. 3a–c), clearly increases with the Mg/Al ratio, dried Mg_2Al showing the smallest value. *Pseudomonas* sp. sorption shows the same tendency on undried products but the adsorption capacities of these latter materials are at least 3 times larger than for dried samples (Fig. 3d), 100% of cells were sorbed at concentrations up to 0.875×10^{10} mL^{-1}. The largest adsorption capacity (160×10^{11} cells/g of solid) demonstrated a fresh suspension of Mg_4Al. The great enhancement of *Pseudomonas* sp. affinities for undried products can be easily related to both the increase of the zeta-potential values and the decrease of particle size of the samples (Table 1).

Adsorption isotherms of cells for dried and undried LDHs and dried LDH–HA complexes (500 mg/L) are given in Fig. 3. All isotherms belong to the H-type, *i.e.* cells have a high affinity for supports. For dried LDHs (Fig. 3a–c) at low cell concentrations ($0.125–0.375 \times 10^{10}$ mL^{-1}), 100% of cells were sorbed; when the cell concentration increased ($0.375–1.250 \times 10^{10}$ mL^{-1}), isotherms showed a plateau corresponding to the saturation stage, as stated by the Langmuir model for molecular adsorption. The adsorption capacity, determined at the plateau (Fig. 3a–c), clearly increases with the Mg/Al ratio, dried Mg_2Al showing the smallest value. *Pseudomonas* sp. sorption shows the same tendency on undried products but the adsorption capacities of these latter materials are at least 3 times larger than for dried samples (Fig. 3d), 100% of cells were sorbed at concentrations up to 0.875×10^{10} mL^{-1}. The largest adsorption capacity (160×10^{11} cells/g of solid) demonstrated a fresh suspension of Mg_4Al. The great enhancement of *Pseudomonas* sp. affinities for undried products can be easily related to both the increase of the zeta-potential values and the decrease of particle size of the samples (Table 1).

The effect of particle size appears to explain such a trend. Two sub-fractions of Mg_4Al with different particle sizes (<2 μm and >2 μm) were prepared and their cell adsorption capacities were compared with the bulk precursor (Supporting information, Fig. S2). All three isotherms are also of H-type. Adsorption capacity of bulk precursor was 41×10^{11} cell/g (mean) and (maximal). The same values were obtained for >2 μm fraction. While for <2 μm fraction mean adsorption capacity was 52×10^{11} cell/g and maximal – 67×10^{11} cell/g of solid. Based on the data, two main conclusions can be made: (i) isotherms of sub-fractions are more distinct and reproducible compared with the noisier one obtained with the bulk product; (ii) adsorption is larger on fine particles (<2 μm) as observed for undried samples.

Such a correlation between adsorption and physico-chemical properties is less obvious for dried samples, due to their greater heterogeneity. While particle size increases with *R*, adsorption capacity also increases. The maximum adsorption uptake increases in the series $Mg_2Al < Mg_3Al < Mg_4Al$. This behavior suggests that interactions with bacteria probably modify their aggregation state. Obviously, dried Mg_4Al retains its aggregation state when resuspended in pure water but when in contact with bacteria, it probably de-aggregates more efficiently and leads to higher adsorption capacity.

Results of *Pseudomonas* sp. adsorption by Mg_3Al LDH–HA complexes with different HA contents are presented in Fig. 3c. Except for Mg_3Al–20%HA that exhibits a desorption phenomenon at high cell concentration (>25×10^{11} g^{-1}), the two other organoclays display also H-type adsorption isotherms. Mean adsorption capacities of LDH–HA complexes were 2–6 times smaller compared with precursors, the adsorption capacity being the smallest for Mg_2Al–10%HA. The observed general tendency is a decrease of cell adsorption due to the presence of HA. Adsorbed HA tremendously modifies the surface properties of LDH as shown by the great change in ζ values and leading to negatively surface charged solids (Table 1). The increase of HA percentage had no visible influence on *Pseudomonas* sp. adsorption despite the observed differences of LDH–HA complex properties (Table 1). At a low LDH surface coverage of 2%HA, LDH–HA nanocomposites are already strongly aggregated and adsorption capacity toward cells is irremediably affected.

3.3. *Statistics*

Table 2 gives the correlation matrix of the data obtained. Adsorption capacity of the studied LDHs and their HA complexes best correlates with their zeta-potentials. Good positive correlation was also obtained with Mg/Al ratio of LDH and good negative correlation with the content of HA.

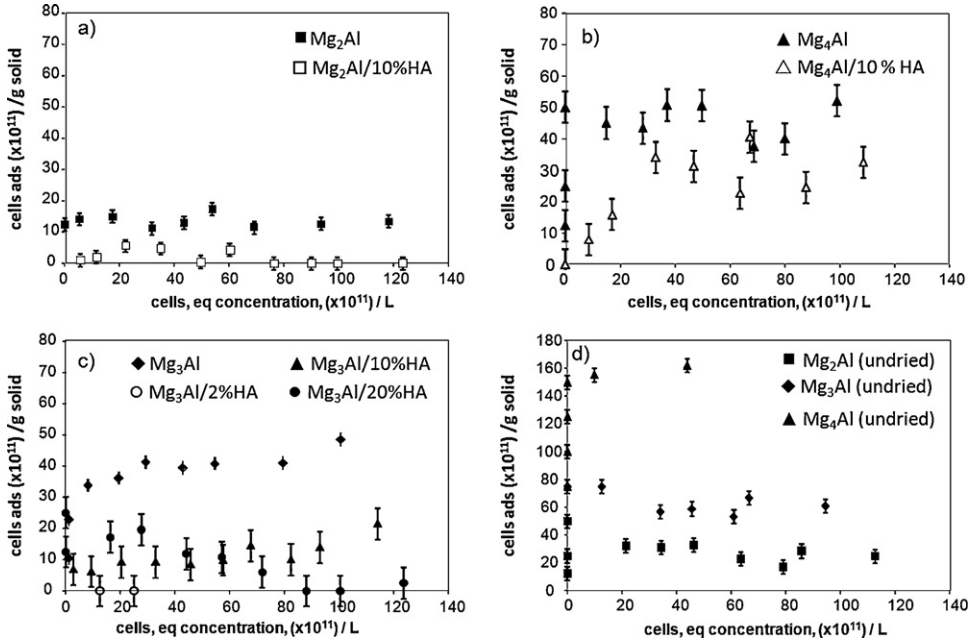

Fig. 3. Isotherms of *Pseudomonas* sp. adsorption on LDH and LDH–HA with different Mg/Al ratio (A) Mg_2Al, (B) Mg_4Al, (C) Mg_3Al and (D) undried LDHs.

3.4. Characterization of Pseudomonas sp. strain ADP/LDH adhesion

As shown by PXRD analyses (Fig. 4a), cell adsorption does not affect strongly the structure of the inorganic solids. Mg_3Al and *Pseudomonas* sp.-Mg_3Al display nearly the same diffraction pattern; a minor enlargement of the diffraction lines is observed for the bionanocomposite, accounting for a slight loss of structural cohesion of the stacked LDH platelets.

FT-IR spectra of cells, Mg_3Al and *Pseudomonas* sp.-Mg_3Al bionanocomposite (25×10^{11} cells/g LDH) are given in Fig. 4b. The IR-spectrum of the bionanocomposite (Fig. 4b, iii) displays, besides the typical vibration bands of Mg_3Al ($\nu_3(NO_3) = 1384\ cm^{-1}$, $\nu_1(NO_3) = 826\ cm^{-1}$, $\delta(HOH) = 1623\ cm^{-1}$, $\delta(MOH) = 839\ cm^{-1}$, $\nu(MO) = 633\ cm^{-1}$ and $\delta(OMO) = 411\ cm^{-1}$), several new adsorption bands at $2930\ cm^{-1}$ ($\nu(CH_2)$ not shown), $1656\ cm^{-1}$ ($\nu(CO)$ amide I), $1536\ cm^{-1}$ ($\nu(NH)$ and $\nu(CN)$ amide II), $1234\ cm^{-1}$ ($\nu(NH)$ and $\nu(CN)$ amide III, skeleton stretching) corresponding to the typical infrared feature of lipids and proteins and at $1083\ cm^{-1}$, the $\nu(CO)$ stretching band of polysaccharides, as observed for free cells (Fig. 4b, i). The $\nu(OH)$ stretching band of H_2O molecules is much larger and intense because of a higher hydration degree. One must notice the clear decrease of the $\nu_3(NO_3)$ band intensity after cell adsorption due to a partial anion exchange of nitrate by anionic residues of the outer cell surface. Recently, Rong et al. [13,14] observed a shift of the $\delta(HOH)$ band to higher frequency for kaolinite, montmorillonite and goethite modified by *Pseudomonas putida* and concluded as a probing effect for cell adhesion onto the clay surface. Such a shift is difficult to detect under the amide I and amide II infrared features, in our case. However, the shift of the $\nu(MO)$ position from 630 to $660\ cm^{-1}$ indicates a clear structural effect of surface adsorption onto LDH platelets. This shift could be assigned to the presence of polyvalent cations which could participate in bioadhesion, probably *via* biopolymers on the outer surface of *Pseudomonas* sp. Such a role of polyvalent cations–polymer interactions in bioadhesion of *Pseudomonas aeruginosa* strains to glass and metal-oxide surfaces was already proposed by Li and Logan [7].

TEM images of *Pseudomonas* sp.-Mg_2-LDH bionanocomposites obtained at different cell concentrations are given in Fig. 5. At low cell concentration ($12.5 \times 10^{11}\ g^{-1}$), the *Pseudomonas* sp. cells (see arrows) create a monolayer biofilm (Fig. 5A) on the surface of the "sand roses" aggregates. In increasing the cell concentration, most of the Mg_2Al particles participate to larger aggregates (Fig. 5B) inside which the cells seem to be embedded (Fig. 5C). Strikingly, a further increase of the cell concentration ($250 \times 10^{11}\ g^{-1}$) induced the formation of multilayered biofilms leading to an unusual architecture based on a cell corona (see arrows) distributed around large LDH aggregates (Fig. 5C).

With the Mg_3Al and Mg_4Al LDH matrices, the TEM observations are quite different (Fig. 6). At low cell concentration ($12.5 \times 10^{11}\ g^{-1}$), they evidence the presence of cells (see arrows) in interaction with the Mg_3Al inorganic phase (Fig. 6A), whereas no cell can be visualized by TEM for Mg_4Al (Fig. 6C). Obviously, the formation of a monolayer biofilm as previously described for Mg_2Al, does not occur for these two different LDH compositions. However for both (Fig. 6B and D), the increase of the cell concentration ($250 \times 10^{11}\ g^{-1}$) favours also the formation of larger aggregate as for Mg_2Al. The thin platelets morphology of the Mg_4Al particles permits to clearly evidence the presence of cells within the aggregates conjointly with cells at the aggregate periphery (see arrows Fig. 6D).

Table 2
Correlation matrix of statistical analysis of data.

	Mg/Al	HA, %	Size	ζ	Ads capacity, %
Mg/Al	1.00	−0.24	0.25	0.07	0.57
HA, %	−0.24	1.00	−0.30	−0.78	−0.58
Size	0.25	−0.30	1.00	0.10	0.03
ζ	0.07	−0.78	0.10	1.00	0.79
Ads capacity, %	0.57	−0.58	0.03	0.79	1.00

3.5. Effect of Pseudomonas sp.-LDH and LDH–HA complex adhesion on atrazine biodegradation

The biodegradation of AT by *Pseudomonas* sp. ADP was carried out in the presence of different quantities of LDH (10, 25, 50, 75 and 100 mg/mL). Fig. 7 presents two examples of kinetics in the

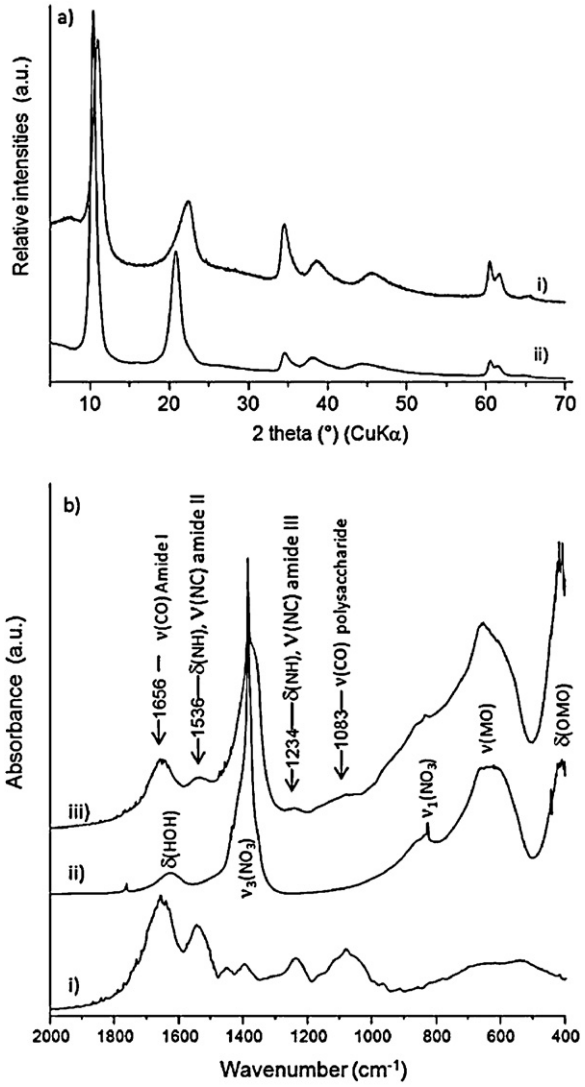

Fig. 4. (A) PXRD of (i) Mg_3Al association with cells (25×10^{11} cells/g), (ii) Mg_3Al and (B) FT-IR spectra of (i) cells, (ii) Mg_3Al and (iii) Mg_3Al association with cells (25×10^{11} cells/g).

absence or presence of Mg_RAl LDH (Supporting information, Fig. S3A). LDH boosted the biodegradative activity of the bacterium whatever their quantity, although no sorption of AT occurred on these solids, the concentration found at T_0 corresponding to the expected one. However considering kinetics to be of first order, the increase of the biodegradation rate depends on the LDH type and on its quantity (Table 3 and Fig. 8A). For Mg_2Al, a linear correlation ($r = 0.987$) was obtained, the more the adsorbent quantity, the higher the biodegradation speed. A maximum factor rate of 26 was reached for Mg_2Al suspension of 100 mg/mL. For Mg_3Al and Mg_4Al, the maximum was obtained with 75 and 50 mg of LDH/mL, respectively. According to the clay quantity, the biodegradation rate increase varied with the layer composition of LDH following: $Mg_2Al < Mg_3Al < Mg_4Al$ for LDH quantity lower than 50 mg/mL. Once Mg_4Al reached its maximum value, its biodegradation efficiency is inverted ($Mg_4Al < Mg_3Al < < Mg_2Al$). The undried products were also tested in the case of Mg_2Al and Mg_4Al at the lowest quantity (10 mg/mL) (Fig. 7 and Supporting information, Fig. S3B). They have a stronger effect on the biodegradation kinetics than dried LDHs, increasing the rate even at low LDH concentration from moderate to a great extent (for example from a factor of 2.5 for Mg_4Al to a factor of 12 for Mg_2Al in the case of 10 mg LDH/mL).

Table 3
Kinetical parameters of atrazine biodegradation by *Pseudomonas* sp. strain ADP and *Pseudomonas* sp. strain ADP–LDHs.

	Clay quantity (mg/mL)	k (h^{-1})	r	Multiplying factor of AT biodegradation rate *vs* cells alone
Cells		0.055	0.987	1.0
	10	0.058	0.979	1.1
	25	0.362	0.992	6.6
Mg_2Al	50	0.781	0.989	14.2
	75	1.230	0.997	22.4
	100	1.460	0.979	26.5
	10	0.203	0.983	3.7
	25	0.313	0.979	5.7
Mg_3Al	50	0.439	0.996	8.0
	75	0.661	0.999	12.0
	100	0.638	0.999	11.6
	10	0.397	0.997	7.2
	25	0.588	0.989	10.7
Mg_4Al	50	0.820	0.989	14.9
	75	0.429	0.967	7.8
	100	0.343	0.992	6.2
Mg_3Al–2%HA	50	0.255	0.990	5.1
Mg_3Al–8%HA	50	0.066	0.985	1.3
Mg_3Al–20%HA	50	0.050	0.997	1.0

To gain better insight on the improvement of the biodegradation, complementary experiments of AT biodegradation were carried out in the presence of the different ions (NO_3^-, Mg^{2+}, Al^{3+}) potentially released into the medium from LDH due to their dissolution equilibrium. A wide range of concentrations of KNO_3 and

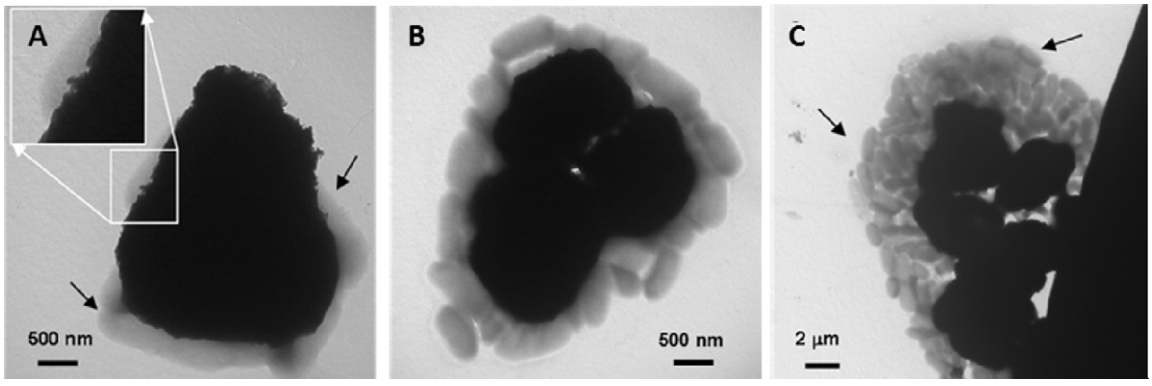

Fig. 5. TEM images of *Pseudomonas* sp. ADP–Mg_2Al LDH at (A) low cell concentration (12.5×10^{11} g^{-1}), (B) intermediate cell concentration (12.5×10^{11} g^{-1}) and (C) excess of cells (250×10^{11} g^{-1}). Cells and cell colonies are indicated with arrows.

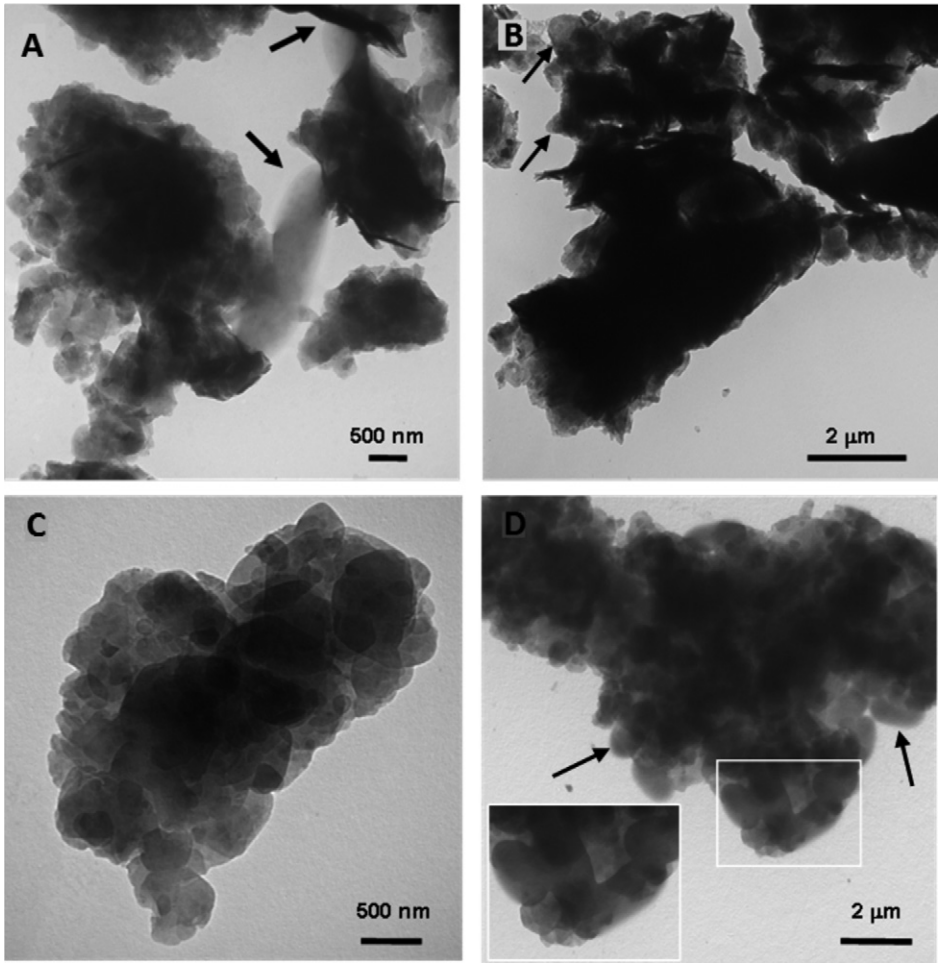

Fig. 6. TEM images of (A and B) *Pseudomonas* sp. ADP–Mg_3Al, and (C and D) *Pseudomonas* sp. ADP–Mg_4Al, obtained respectively at low (12.5×10^{11} g^{-1}) and high (250×10^{11} g^{-1}) cell concentrations. Cells and cell colonies are indicated with arrows.

$MgCl_2$ (10–100 mM) were tested for the effect on biodegradation. Biodegradation experiments were also carried out under similar conditions (1–50 mg/mL) with $Mg(OH)_2$ and $Al(OH)_3$ considered as analogous layered metal hydroxides often encountered in the <2 μm soil fractions. No significant effect on the biodegradation rate was observed. The supernatant, obtained after centrifugation of a 24 h-stirring period of the different LDHs in water, was also used as incubation medium for AT biodegradation. The biodegrada-

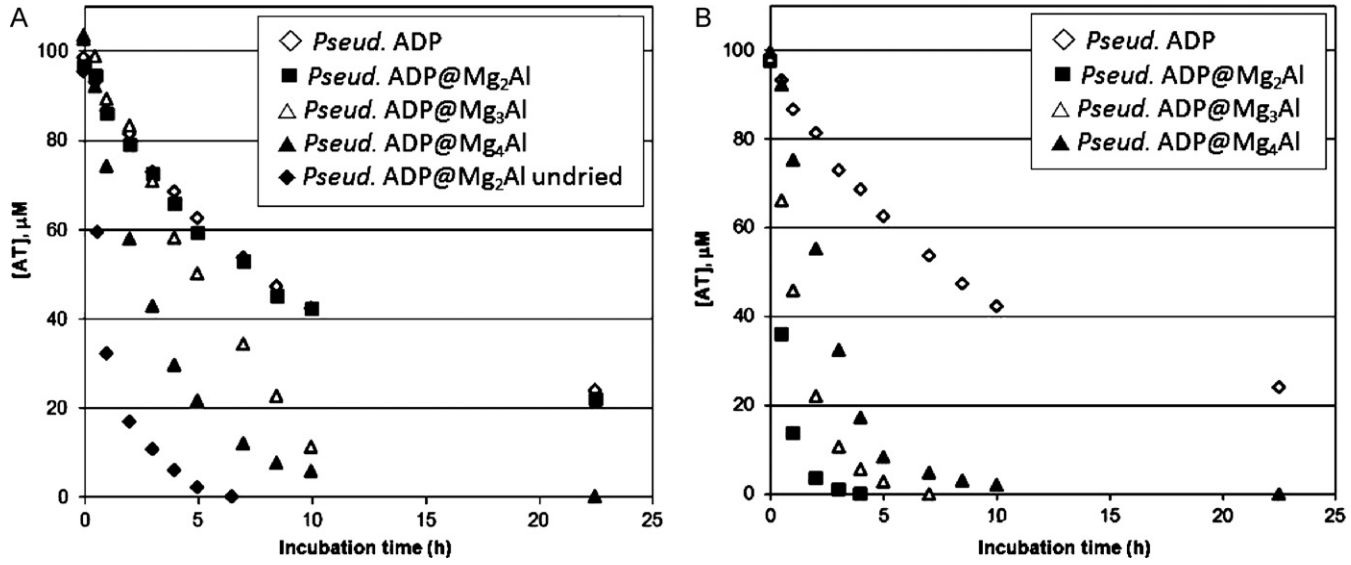

Fig. 7. Biodegradation of AT (100 μM) by *Pseudomonas* sp. ADP and *Pseudomonas* sp. ADP–Mg_RAl at (A) 10 mg/mL and (B) 100 mg/mL of solid. Mean values from 3 independent experiments in each case.

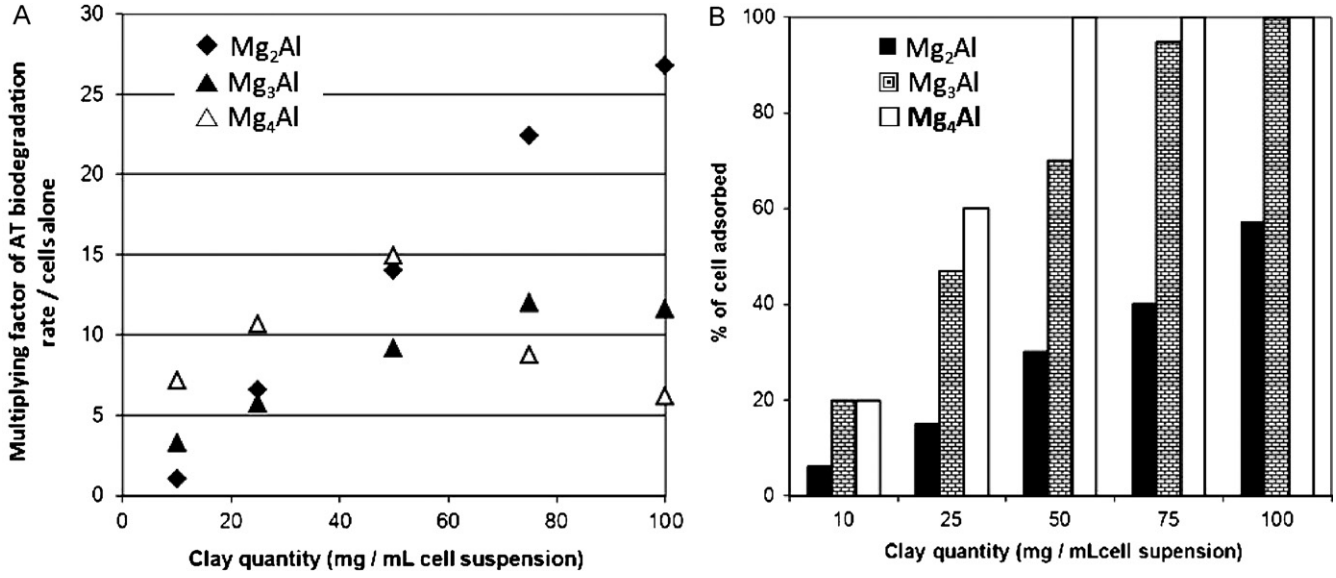

Fig. 8. (A) Multiplying factor in the biodegradation rate of *Pseudomonas* sp. ADP–Mg_RAl *vs* cells alone and (B) adsorbed cell percentage *vs* Mg_RAl LDH amounts at similar cell concentration than for biodegradation study.

tion curve obtained was completely superimposed on that obtained under standard conditions (free cells) in water (data not shown). These results confirm that the increase of the biodegradative activity toward AT were really due to the interaction between the bacteria and the LDH matrices.

The adsorption of *Pseudomonas* sp. on LDH–HA complexes lead to some improvements of the bioactivity toward AT degradation, in particular with low HA content. However, this positive effect (increase of the biodegradation rate) was lower than with pure LDH and decreased with HA mass loading increased (Table 3 and Supporting information, Fig. S3C). This phenomenon correlated also with the percentage of AT adsorbed on the solid matrix. In these cases, two processes took place: sorption of both the substrate (observed at T_0) and the bacterial cells.

4. Discussion

4.1. Cell adsorption

Bacteria adsorption on LDHs–NO_3 and their HA complexes is very fast: 90% of cells were adsorbed in less than 5 min. The adsorption capacities of Mg_RAl LDH toward *Pseudomonas* sp. cells are high, 45.5×10^{11} g^{-1} for Mg_4Al, for example. For all the series, adsorption capacity increased as Mg/Al ratio increased. The values obtained are at least one order of magnitude larger than Mg_2Al-Cl efficiencies previously reported [25,34]. Compared with other sorption materials (clay minerals, metal oxides/hydroxides, activated carbon), LDHs demonstrate exceptional higher adsorption capacities [25]. Surface modification of LDH by HA leads to a noticeable reduction of the cell adsorption.

In terms of an adhesion mechanism, electrostatic interactions between bacteria and LDH platelet surface seem to play a key role, as testified by the good correlations between adsorption efficiencies and either zeta-potential values ($R^2 = 0.79$) or HA loading ($R^2 = -0.58$). Nevertheless, cell adsorption does not increase simplistically with LDH structural surface charge from Mg_4Al to Mg_2Al, as it should be expected but it is more related to macroscopic properties of the solids and particularly, ζ value. Zeta-potential does not directly account for the structural charge but depends much on the electric potential at the surface of particles and consequently on the nature of particle aggregation as observed. The effect of Mg/Al ratio of LDH on bacteria adsorption is the most surprising and differences in their Zeta-potential can explain this effect only partly; $\zeta = -19 \pm 3$ mV for *Pseudomonas* sp. ADP cells against +6.1 mV < ζ < +12 mV for dried LDHs. It is interesting to note that brucite and gibbsite samples which display positive zeta values adsorbed fewer amounts of cells and did not affect favourably the biodegradation kinetics of *Pseudomonas* sp. (data not shown). Surprisingly, major differences in adsorption capacities of undried products cannot account only for changes in electrochemical surface properties since they exhibit similar zeta-potential values (Table 1). These results evidence that other parameters have to be considered in the process, such as the accessible surface area of fresh suspended LDH particles. Obviously, particle size and aggregation state also affect strongly the adsorption capacities of LDH for cells. With homogeneous LDH fresh suspensions, a logical increase of cell adsorption with particle size decreasing is observed. Drying irreversibly changes LDH properties which limit surface adsorption.

Additionally, from a mechanistic point of view, H-bonds contribute strongly to cell adsorption. Indeed proteins have a strong affinity for all types of surface [35–37]. This versatile affinity originates from the diversity of aminoacids that can be classified as positively, neutrally or negatively charged and from hydrophobic properties [38] which range from polar (hydrophilic) to non-polar. These properties give rise to a wide variety of interactions with mineral surfaces. For instance, aspartate and glutamate aminoacid residues containing proteins and OH-groups of polysaccharide compounds may help to anchorage the cells to the positively charged hydroxylated surface of LDH. Also, polyvalent metal bridging probably contributes to adsorption due to the polymers on the outer surface of the bacterium, frequently carrying a negative charge.

In the presence of HA, other forces prevail. We assume that HA molecules do not create a continuous coverage of the LDH particles but rather exist as adsorbed clusters with a multilayered structure developing hydrophobic domains favourable to AT adsorption but letting some remaining LDH surface domains free for cell adsorption. This adsorption occurs then at the remaining bare hydrophilic hydroxylated LDH surface. The Mg_RAl–HA behavior may then be explained by both a masking effect of the overall positive charges

of the layers and a reduction of the specific surface area due to surface adsorption of the biopolymer. No big differences have been observed on higher HA loading from 2% to 20% in case of Mg_3Al–AH. Although the effect of HA adsorption by LDH on bacteria interaction has not been previously discussed in literature, similar trends have been found for other mineral surfaces [11,39]. In a recent study on *Escherichia coli* attachment on different agricultural soils, Guber et al. [39] showed that cell adsorption isotherms follow a linear behavior. Adsorption capacities on these soils fell within the range of 13.9–48.2 10^4 CFU g^{-1} (CFU for colony-forming units). *E. coli* attachment to soils was by the presence of manure. Increasing its content generally decreased attachment.

4.2. Cell biodegradation activity enhancement

It has been reported that bacterial attachment to the support could greatly influence in a positive or negative way the microbial metabolic activity [20,40]. Our results showed clearly that favourable adsorption of *Pseudomonas* sp. cells at the LDH surface, preferential to self-assembling, increases greatly the bacterial biodegradative activity for AT, a non-sorbed substrate. This phenomenon is really due to the specific physico-chemical properties of the anionic clay surface itself since no significant effect of LDH constitutive ions on the biodegradation kinetics was demonstrated.

Nevertheless the effect was greatly dependent on both the Mg/Al ratio and the LDH quantity. The maximal enhancing effect was obtained with 100% of cells adsorbed on Mg_3Al and Mg_4Al and with the highest cell adsorption rate for Mg_2Al (Fig. 8). The formation of a monolayer biofilm for Mg_2Al was the most effective even in a case of limited cell adsorption capacity of this product. This intimate adhesion of cells on the entire surface of LDH particles favoured the atrazine biodegradation. Several hypotheses can be proposed to explain that: presence of an optimized local pH for the bacterial activity due to the buffering capacity of clays (around pH 8.5), changes in the structure and permeability of the membranes due to adhesion, hindrance of AT adsorption by cell due to compact biofilm formation. When the cell/solid ratio increased, multilayered biofilms of bacterial cells were formed and the effect on atrazine biodegradation was at a lower extent, certainly due to substrate diffusion problem.

This acceleration effect was lost, with more LDH–HA complex present and higher HA percentage. LDH–HA organoclays display also significant kinetical effect on AT biodegradation. However, modification of LDH surface by HA complexation reduced up to 6 times the cell adsorption compared to bare LDH. The sorption surface sites were occupied by HA and interactions between bacterial cells and LDH were no longer or less favoured. Conversely, sorption process of AT on LDH–HA complexes occurred in a greater or lesser extent depending on the content of HA and the type of LDH. It was therefore difficult to correctly attribute the effect loss on biodegradation to one or the other phenomenon.

5. Conclusion

In conclusion, adhesion of bacterial cells on a LDH matrix can greatly influence the metabolic activity of contaminant biodegradation even in the case of non-sorbed contaminant. A great enhancement of AT biodegradation kinetics was observed due to the formation of *Pseudomonas* sp. ADP–MgAl bionanocomposites. This beneficial effect depends on both the quantity and properties of the LDH solid (Mg^{2+}/Al^{3+} ratio; presence or absence of HA) and also on the architecture of the bacterial biofilm formed. The obtained results make this type of synthetic products with their unique structure an ideal and promising solid for microbiological applications. Ex situ bioremediation of atrazine contaminated water by *Pseudomonas* sp.-Mg_RAl could then be envisaged favourably. Use of LDHs as mineral supports for cells will be extended to other bacteria and biodegradation of other xenobiotics.

Acknowledgements

T. Alekseeva thanks the CNRS for the invited researcher position. Dr Hans-Peter Buser from Syngenta Crop Protection AG (Basel, Switzerland) is gratefully acknowledged for the gift of atrazine standard.

Appendix A. Supplementary data

Supplementary data associated with this article can be found, in the online version, at doi:10.1016/j.jhazmat.2011.04.050.

References

[1] M. Nazare, P.F.S. Couto, E. Monteiro, M. Teresa, S.D. Vasconcelos, Mesocosm trials of bioremediation of contaminated soil of a petroleum refinery: comparison of natural attenuation, biostimulation and bioaugmentation, Environ. Sci. Pollut. Res. 17 (2010) 1339–1346.
[2] S. El Fantroussi, S.N. Agathos, Is biaugmentation a feasible strategy for pollutant removal and site remediation? Curr. Opin. Microbiol. 8 (2005) 268–275.
[3] S.H. Streger, S. Vainberg, H. Dong, P.B. Hatzinger, Enhancing transport of *Hydrogenophaga flava* ENV735 for bioaugmentation of aquifers contaminated with methyl *tert*-butyl ether, Appl. Environ. Microbiol. 68 (2002) 5571–5579.
[4] M.E. Parent, D. Velegol, *E. coli* adhesion to silica in the presence of humic acid, Colloid Surf. B 39 (2004) 45–51.
[5] C. Vettori, G. Stotzky, M. Yoder, E. Gallori, Interaction between bacteriophage PBS1 and clay minerals and transduction of *Bacillus subtilis* by clay-phage complexes, Environ. Microbiol. 1 (1999) 347–355.
[6] M. Katsikogianni, Y.F. Missirlis, Concise review of mechanisms of bacterial adhesion to biomaterials and of techniques used in estimating bacterial–mineral interactions, Eur. Cells Mater. 8 (2004) 37–57.
[7] B. Li, B.E. Logan, Bacterial adhesion to glass and metal-oxide surfaces, Colloid Surf. B 36 (2004) 81–90.
[8] H.C. Kim, S.J. Park, C.G. Lee, S.B. Kim, K.W. Kim, Bacterial attachment to iron-impregnated granular activated carbon, Colloid Surf. B 74 (2009) 196–201.
[9] A. Jacobs, F. Lafolie, J.M. Herry, M. Debroux, Kinetic adhesion of bacterial cells to sand: cell surface properties and adhesion rate, Colloid Surf. B 59 (2007) 35–45.
[10] C.G. Lee, S.J. Park, Y.U. Han, J.A. Park, S.B. Kim, Bacterial attachment and detachment in aluminium-coated quartz sand in response to ionic strength change, Water Environ. Res. 82 (2010) 499–505.
[11] R.L. Richardson, A.L. Mills, J.S. Herman, G.M. Hornberger, Effect of humic material on interactions between bacterial cells and mineral surfaces, LMECOL Contribution, University of Virginia 01 (2000) 1–7.
[12] D. Jiang, Q. Huang, P. Cai, X. Rong, W. Chen, Adsorption of *Pseudomonas putida* on clay minerals and iron oxide, Colloid Surf. B 54 (2007) 217–221.
[13] X. Rong, Q. Huang, X. He, H. Chen, P. Cai, W. Liang, Interaction of *Pseudomonas putida* with kaolinite and montmorillonite: a combination study by equilibrium adsorption, ITC, SEM and FTIR, Colloid Surf. B 64 (2008) 49–55.
[14] X. Rong, W. Chen, Q. Huang, P. Cai, W. Liang, *Pseudomonas putida* adhesion to goethite: studied by equilibrium adsorption, SEM, FTIR and ITC, Colloid Surf. B 80 (2010) 79–85.
[15] T. Missana, A. Adell, On the applicability of DLVO theory to the prediction of clay colloids stability, J. Colloid Interf. Sci. 230 (2000) 150–156.
[16] H.H.M. Rijnaarts, W. Norde, J. Lyklema, A.J.B. Zehnder, DLVO and steric contributions to bacterial deposition in media of different ionic strengths, Colloid Surf. B 14 (1995) 179–195.
[17] M.C.M. Van Loosdrecht, J. Lyklema, W. Norde, A.J.B. Zehnder, Influence of interfaces on microbial activity, Microb. Rev. 54 (1990) 75–87.
[18] C. Chenu, G. Stotzky, Interactions between microorganisms and soil particles: an overview, in: P.M. Huang, J.M. Bollag, N. Senesi (Eds.), Interactions Between Soil Particles and Microorganisms: Impact on the Terrestrial Ecosystems, IUPAC Series on Analytical and Physical Chemistry on Environmental Systems, vol. 8, Wiley & Sons, 2002, pp. 9–17 (Chap. 1).
[19] H. Chen, X. He, X. Rong, W. Chen, P. Cai, W. Liang, S. Li, Q. Huang, Adsorption and biodegradation of carbaryl on montmorillonite, kaolinite and goethite, Appl. Clay Sci. 46 (2009) 102–108.
[20] P. Cai, X. He, A. Xue, H. Chen, Q. Huang, J. Yu, X. Rong, W. Liang, Bioavailability of methyl parathion adsorbed on clay minerals and iron oxide, J. Hazard. Mater. 185 (2011) 1032–1036.
[21] N. Massalha, S. Basheer, I. Sabbah, Effect of adsorption and bead size of immobilized biomass on the rate of biodegradation of phenol at high concentration levels, Ind. Eng. Chem. Res. 46 (2007) 6820–6824.
[22] J.H. Park, Y. Feng, P. Ji, T.C. Voice, S.A. Boyd, Assessment of bioavailability of soil-sorbed atrazine, Appl. Environ. Microbiol. 69 (2003) 3288–3298.

[23] P. Leglize, A. Saada, J. Berthelin, C. Leyval, Adsorption of phenanthrene on activated carbon increases mineralization rate by specific bacteria, J. Hazard. Mater. 151 (2008) 339–347.
[24] P. Besse-Hoggan, T. Alekseeva, M. Sancelme, A.M. Delort, C. Forano, Atrazine biodegradation modulated by clays and clay/humic acid complexes, Environ. Pollut. 157 (2009) 2837–2844.
[25] S. Jin, P.H. Fallgren, J.M. Morris, Q. Chen, Removal of bacteria and viruses from waters using layered double hydroxide nanocomposites, Sci. Technol. Adv. Mater. 8 (2007) 67–70.
[26] C. Forano, T. Hibino, F. Leroux, C. Taviot-Gueho, Layered Double Hydroxides, in: F. Bergaya, B.K.G. Theng, G. Lagaly (Eds.), Handbook of Clay Science (Developments in Clay Science), vol. 1, Elsevier, 2006 (Chap. 13.1).
[27] A. Hall, M. Stamatakis, Hydrotalcite and an amorphous clay mineral in high-magnesium mudstones from the Kozani basin, Greece, J. Sediment. Res. 70 (2000) 549–558.
[28] E.J. Elzinga, D.L. Sparks, Reaction condition effects on nickel sorption mechanisms in illite–water suspensions, Soil Sci. Soc. Am. J. 65 (2001) 94–101.
[29] F. Juillot, G. Morin, P. Ildefonse, T.P. Trainor, M. Benedetti, L. Galoisy, G. Calas, G.E. Brown, Occurrence of Zn/Al hydrotalcite in smelter-impacted soils from northern France: evidence from EXAFS spectroscopy and chemical extractions, Am. Mineral. 88 (2003) 509–526.
[30] G. Grünewald, K. Kaiser, R. Jahn, Soil development and alteration of secondary minerals along a time series in alkaline soils derived from carbonatic wastes of soda production, Catena 71 (2007) 487–496.
[31] G. Grünewald, K. Kaiser, R. Jahn, Hydrotalcite – a potentially significant sorbent of organic matter in calcareous alkaline soils, Geoderma 147 (2008) 141–150.
[32] A. de Roy, C. Forano, J.P. Besse, Layered Double Hydroxides: synthesis and post-synthesis modifications, in: V. Rives (Ed.), Layered Double Hydroxides: Present and Future, Nova Science Publishers Inc., New York, 2001, pp. 1–37.
[33] Z. Chang, D.G. Evans, X. Duan, C. Vial, J. Ghanbaja, V. Prevot, M.E. de Roy, C. Forano, Synthesis of [Zn-Al-CO_3] layered double hydroxides by a coprecipitation method under steady-state conditions, J. Solid State Chem. 178 (2005) 2766–2777.
[34] Y. You, G.F. Vance, D.L. Sparks, J. Zhuang, Y. Jin, Sorption of MS2 bacteriophage to Layered Double Hydroxides: effects of reaction time, pH, and competing anions, J. Environ. Qual. 32 (2003) 2046–2053.
[35] C. Forano, S. Vial, C. Mousty, Nanohybrid enzymes–Layered Double Hydroxides: potential applications, current nanoscience, CNANO, Trends Bio-hybrid Nanostruct. Mater. 2 (2006) 283–294.
[36] H. Quiquampoix, R.G. Burns, Interactions between proteins and soil mineral surfaces: environmental and health consequences, Elements 3 (2007) 401–406.
[37] V. Prevot, C. Forano, Bio-inorganic hybrids based on enzyme, in: E. Ruiz-Hitzky, K. Ariga, Y.M. Lvov (Eds.), Bio-Inorganic Hybrid Nanomaterials: Strategies, Syntheses, Characterization and Applications, Wiley Publisher, 2007, pp. 313–337.
[38] K.M. Biswas, D.R. DeVido, J.G. Dorsey, Evaluation of methods for measuring amino acid hydrophobicities and interactions, J. Chromatogr. A 1000 (2003) 637–655.
[39] A.K. Guber, D.R. Shelton, Ya.A. Pachepsky, Effect of manure on *Escherichia coli* attachment to soil, J. Environ. Qual. 34 (2005) 2086–2090.
[40] G. Chen, K.A. Strevett, Impact of surface thermodynamics on bacterial transport, Environ. Microbiol. 3 (2001) 237–245.